BELLE2-NOTE-PL-2022-002
April 20, 2022

Study of photon energy bias using $\pi^0 \to \gamma\gamma$ decays from $D^{*+} \to D^0(\to K^-\pi^+\pi^0)\pi^+$

The Belle II collaboration

We reconstruct clean samples of $\pi^0 \to \gamma\gamma$ decays from the $D^{*+} \to D^0(\to K^-\pi^+\pi^0)\pi^+$ decay chain in both data and simulation to study the bias in the reconstructed π^0 mass. We use the data collected by Belle II during 2019, 2020 and the first half of 2021 which correspond to $207\,\text{fb}^{-1}$ of integrated luminosity. The results from the data are compared to run-dependent and run-independent official Belle II simulations. The study is performed as a function of the photons' energies and polar angles.

1 Introduction

This note presents a data-simulation comparison of the π^0-mass distribution using $\pi^0 \to \gamma\gamma$ decays from the $D^{*+} \to D^0(\to K^-\pi^+\pi^0)\pi^+$ decay chain.[1] The study is meant to inform about data-simulation differences resulting from biases in the measurement of photon energies at Belle II.

The analysis uses e^+e^--collision data collected by Belle II [1] between 2019 and the first half of 2021, which correspond to an integrated luminosity $207\,\text{fb}^{-1}$. Belle II [1], operating at the SuperKEKB [2] asymmetric e^+e^- collider in Japan, consists of several sub detector arranged in a cylindrical structure around the beam pipe. It is designed to detect long-lived charged and neutral particles emitted from SuperKEKB collisions and measure their four-momentum. The innermost detector nearest to the interaction region (IR) is the vertex detector (VXD), which consists of two layers silicon-pixel detector (PXD) and a four-layer double-sided silicon-strip detector (SVD). A central drift chamber (CDC) is located outside of the VXD to track charged particles. Charged-particle identification is provided by a time-of-propagation counter (TOP) and an aerogel ring-imaging cherenkov detector (ARICH) that cover the barrel and forward end-cap regions, respectively. Further out, an electromagnetic calorimeter (ECL) made of thallium-doped cesium-iodide crystals is used to detect energy of photons and to separate electrons from hadrons. The K_L and muon detector (KLM) is the outermost sub-detector to identify K_L^0 mesons and muons.

Simulation events are generated using KKMC [3] for quark-antiquark pairs from e^+e^- collisions, PYTHIA8 [4] for hadronization, EVTGEN [5] for the decay of the generated hadrons, and GEANT4 [6] for the detector response.

2 Event selection

Events enriched in signal $D^{*+} \to D^0(K^-\pi^+\pi^0)\pi^+$ decays are first selected by requiring the presence of at least three tracks with transverse momentum $p_\text{T} > 0.2\,\text{GeV}/c$ and originating from the IR, and by vetoing events consistent with Bhabha scattering. Photon candidates are formed from isolated ECL clusters that are not matched to any track. The cluster polar angle is required to be in the CDC acceptance ($17° < \theta < 150°$), the cluster timing uncertainty must be smaller than 10^6 ns, and the cluster energy must be larger than 75 MeV or the ratio between the energies of the central crystal, E_1, and the 3×3 crystals around the central crystal, E_9, must be larger than 0.4. Two photon candidates are combined to form $\pi^0 \to \gamma\gamma$ decays. The two photons are ordered by polar angle, with the leading photon (γ_1) corresponding to the one with larger polar angle. The two photons are required to have energies within 5% of each other, $|[E(\gamma_1) - E(\gamma_2)]/E(\gamma_1)| < 0.05$, to more easily relate any shift in the π^0 mass position to a bias in the reconstruction of the photon energy [7]. Candidates with π^0 masses in the range $[0.08, 0.2]\,\text{GeV}/c^2$ are then combined with two oppositely charged tracks to form $D^0 \to K^-\pi^+\pi^0$ candidates. The tracks are required to originate from the IR, have at least 20 hits in the CDC and be identified as either a pion ($\mathcal{L}_\pi/(\mathcal{L}_K + \mathcal{L}_\pi) > 0.3$) or a kaon ($\mathcal{L}_K/(\mathcal{L}_K + \mathcal{L}_\pi) > 0.3$), where $\mathcal{L}_K$ and $\mathcal{L}_\pi$ are the likelihoods of kaon and pion, respectively, as determined from the particle-

[1] Charge-conjugate decays are implied throughout.

identification information provided by the CDC, the TOP and the ARICH detectors. The mass of the D^0 candidates is required to be in the range $[1.84, 1.88]\,\mathrm{GeV}/c^2$. The D^0 candidates are combined with low-momentum ("soft") pions to form $D^{*+} \to D^0\pi^+$ candidates. The soft pions are selected from the list of tracks that are in the CDC acceptance, are consistent with originating from the IR and have at least one hit in the CDC. The D^{*+} candidates are fit using `TreeFitter` [8] by constraining the D^{*+} production vertex to the measured position of the IR. The fit must converge and have χ^2-probability in excess of 1%. The momentum of the D^{*+} in the e^+e^- center-of-mass system must exceed $2.3\,\mathrm{GeV}/c^2$ to suppress combinatorial background and events where the D^{*+} originates from a B decay. The difference between the D^{*+} and D^0 masses, Δm, must be in the range $[0.1445, 0.1465]\,\mathrm{GeV}/c^2$. When multiple D^{*+} candidates are selected in the same event, only the one with largest `TreeFitter` probability is kept.

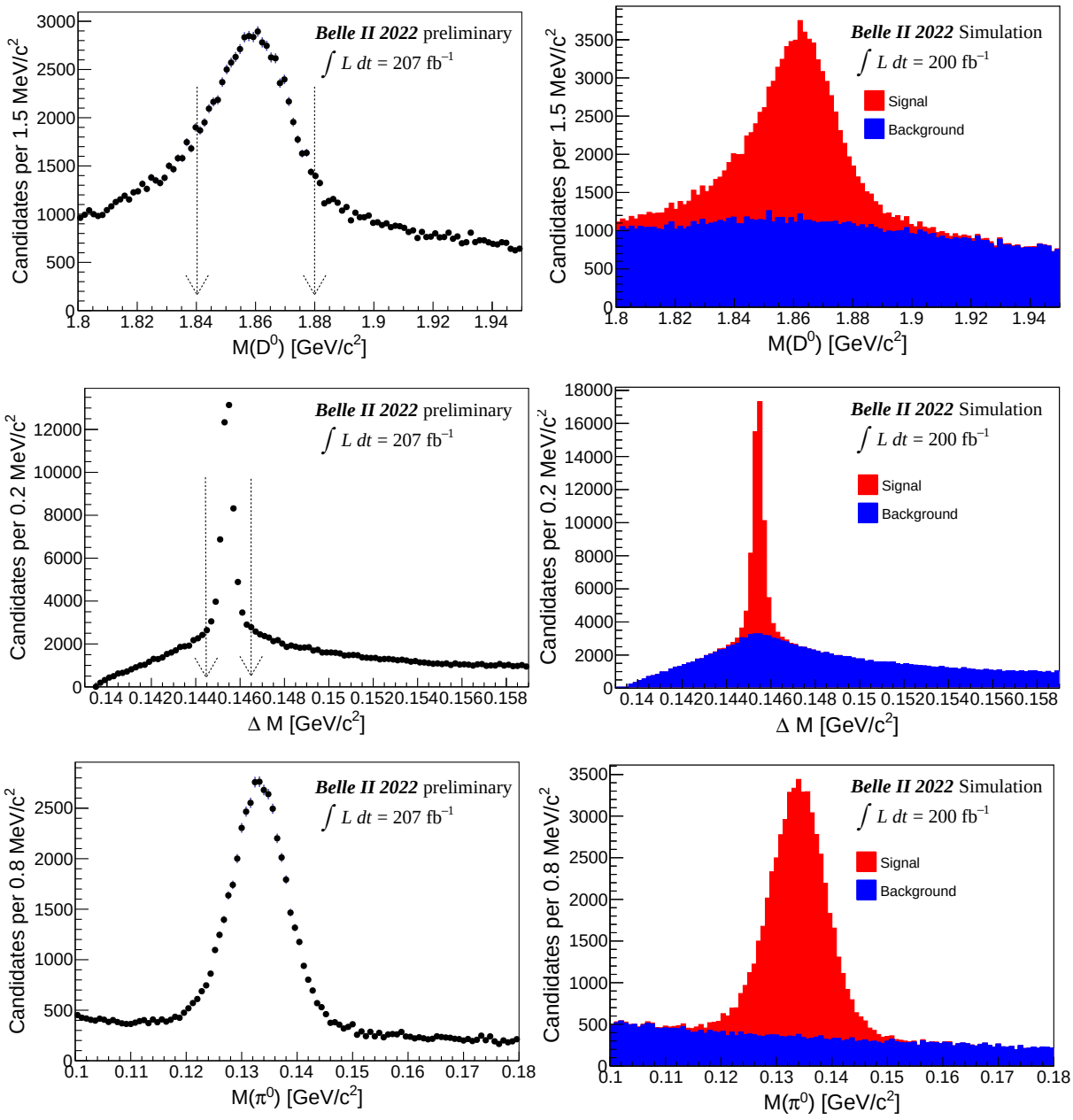

Figure 1: Distribution of (top) $m(D^0)$, (middle) difference between the D^{*+} and D^0 masses (Δm) and (bottom) π^0 mass for $D^{*+} \to D^0(K^-\pi^+\pi^0)\pi^+$ candidates reconstructed in (left) data and (right) simulation. The $m(D^0)$ (Δm) distribution is only for candidates populating the Δm ($m(D^0)$) signal region indicated by the vertical lines. The π^0-mass distribution is only for candidates populating the Δm and Δm signal regions, and after the removal of the events with multiple D^{*+} candidates.

The $m(D^0)$, Δm and π^0 mass distributions of the selected candidates, separately for data and simulation, are shown in Figure 1.

3 Data-simulation comparison

Unbinned maximum-likelihood fits to the π^0-mass distributions from subsets of the data and of the simulation, selected according the leading photon energy or polar angle, are used to determine the variation of the π^0-mass peak position and width as a function of the subsets considered. In each fit, the signal component is described by a Gaussian distribution and the background component by an exponential distribution. Example fits to the π^0-mass distributions of the data in two bins of leading photon energy are shown in Figure 2.

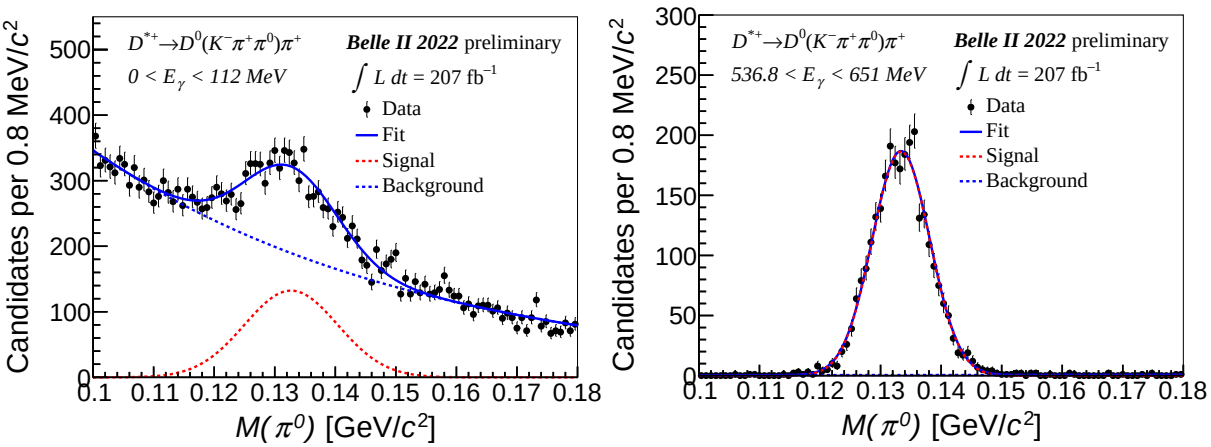

Figure 2: Distribution of $M(\pi^0)$ for $D^{*+} \to D^0(K^-\pi^+\pi^0)\pi^+$ candidates reconstructed in data collected by Belle II during 2019, 2020 and the first half of 2021, and corresponding to an integrated luminosity 207 fb^{-1}, in the lower ($0 < E_\gamma < 112$ MeV: left) and higher ($536.8 < E_\gamma < 651$ MeV: right) bins of leading photon energy for all candidates, with fit projection overlaid. Low mass tail of $M(\pi^0)$ signal is suppressed due to D^0 selection cuts.

The data-simulation ratio between the π^0-mass peak position and width as a function of the leading photon energy for all candidates is shown in Figure 3. We observed the data-simulation ratios of both the π^0-mass peak and the π^0-mass width are within $\approx 1\%$ from unity and approaching 1 for higher energies.

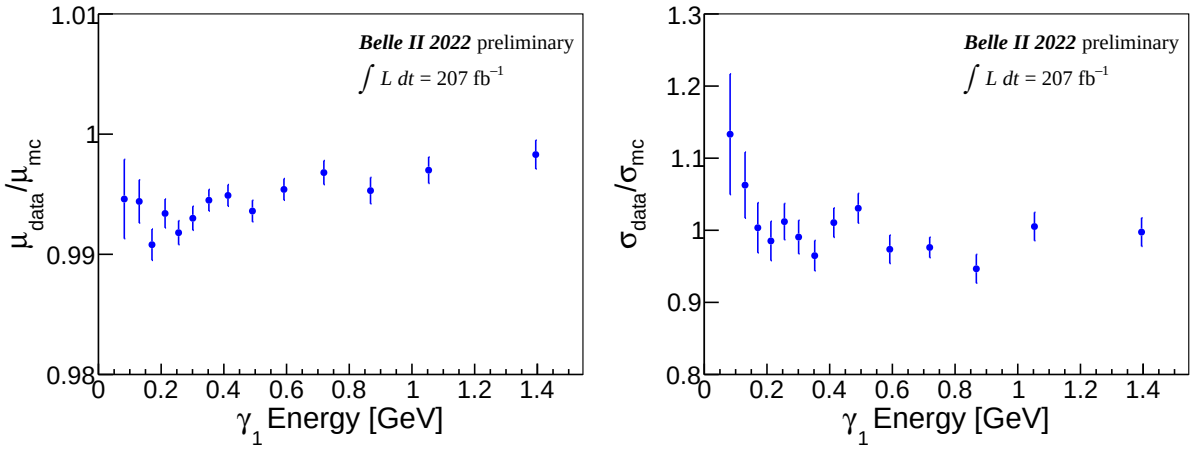

Figure 3: Variation of the data/simulation ratios of (left) mean π^0 mass μ and (right) π^0-mass resolution σ for $D^{*+} \to D^0(K^-\pi^+\pi^0)\pi^+$ candidates as a function of leading photon energy for all candidates.

References

[1] W. Altmannshofer et al., Belle II collaboration, *The Belle II Physics Book*, arXiv:1808.10567 [hep-ex].

[2] K. Akai, K. Furukawa, and H. Koiso, SuperKEKB, *SuperKEKB Collider*, Nucl. Instrum. Meth. **A907** (2018) 188–199, arXiv:1809.01958 [physics.acc-ph].

[3] S. Jadach, B. F. L. Ward, and Z. Was, *The Precision Monte Carlo event generator K K for two fermion final states in e+ e- collisions*, Comput. Phys. Commun. **130** (2000) 260–325, arXiv:hep-ph/9912214 [hep-ph].

[4] T. Sjöstrand, S. Ask, J. R. Christiansen, R. Corke, N. Desai, P. Ilten, S. Mrenna, S. Prestel, C. O. Rasmussen, and P. Z. Skands, *An Introduction to PYTHIA 8.2*, Comput. Phys. Commun. **191** (2015) 159–177, arXiv:1410.3012 [hep-ph].

[5] D. J. Lange, *The EvtGen particle decay simulation package*, Nucl. Instrum. Meth. **A462** (2001) 152–155.

[6] S. Agostinelli et al., *GEANT4—a simulation toolkit*, Nuclear instruments and methods in physics research **506** (2003) 250–303.

[7] U. Tamponi, Belle collaboration, *Study of the η meson transitions from $\Upsilon(4S)$ and $\Upsilon(5S)$ with the Belle Experiment*, inspirehep **2014** (2014) .

[8] J.-F. Krohn et al., Belle II analysis software Group, *Global decay chain vertex fitting at B-factories*, arXiv:1901.11198 [hep-ex].